Quantum chaotic scattering with a mixed phase space: The three-disk billiard in a magnetic field

Markus Eichengrün and Walter Schirmacher
Physik-Department E13, Technische Universität München, D-85747 Garching, Germany

Wolfgang Bregmann
Institut für Physik, Universität Basel, Klingelberstrasse 82 CH-4056 Basel, Switzerland
(Received 2 July 1999)

We study the classical and semiclassical scattering behavior of electrons in an open three-disk billard in the presence of a homogeneous magnetic field, which is confined to the inner part of the scattering region. As the magnetic field is increased the phase space of the invariant set of the classical scattering trajectories changes from hyperbolic (fully chaotic) to a mixed situation, where KAM tori are present. The ''stickiness'' of the stable trajectories leads to a much slower decay of the survival probability of trajectories as compared to the hyperbolic case. We show that this effect influences strongly the quantum fluctuations of the scattering amplitude and cross sections.

PACS number(s): 05.45.−a, 03.65.Sq, 72.20.−i

I. INTRODUCTION

It is fascinating to study the quantum-mechanical scattering properties of mesoscopic systems because this field combines the rather applied topic of device miniaturization [1,2] with the search for quantum traces of classically nonintegrable dynamics [3]. It has, for example, been shown that the quantum fluctuations exhibited by electronic transmission coefficients through mesoscopic cavities are related to the statistics of classical ballistic trajectories by means of the semiclassical approximation [4–6]. One point of interest was to study the quantum correlation functions that correspond to structures whose classical dynamics is fully chaotic or fully integrable [7]. Especially the case of chaotic scattering in which the phase space properties of the trapped periodic orbits (invariant set) play the key role has been addressed [4,8]. It has, in particular, been realized that in the case of a mixed phase space, which is the most important one, the fluctuations differ drastically from those in the two other cases, namely, the fully chaotic and the fully regular situation. This is so, because the stable members of the invariant set hinder the transient orbits to leave the scattering region (''stickiness'' of the stable pinned orbits). Thereby interference patterns are produced that lead to mesoscopic fluctuations with a statistics that is characteristic for the mixed phase space case [9–15].

An interesting chaotic scattering model, in which the invariant set posseses a mixed phase space, is the three-disk billiard in the presence of an applied magnetic field [16]. In the absence of an applied field the scattering from the three-disk billiard is fully chaotic (hyperbolic) [17]. In the presence of a magnetic field the system becomes less chaotic and, beyond a certain critical field stable islands appear in the phase space.

In this article we present a case study of the classical and quantum-mechanical scattering properties of the three-disk billiard with magnetic field. This system is also interesting from an applied point of view, because it can be viewed as the inner part of a rounded three-lead junction. In Sec. II we compare the statistical properties of the scattered trajectories in the nonhyperbolic situation with the field-free hyperbolic case. In Sec. III we investigate the quantum fluctuations of the scattering amplitudes and cross sections in the two cases by means of the semiclassical approximation. We demonstrate in detail, how the fluctuations are influenced by the phase space of the classical invariant set. We further check the validity of various approximations used in the literature for relating the classical statistics to the quantum fluctuations.

II. THE THREE-DISK BILLIARD: CLASSICAL SCATTERING PROPERTIES

We consider an incident beam of classical particles in two dimensions with charge $Q=-e$ and initial momentum $\mathbf{p}=\hbar k\mathbf{e}_x$, which are scattered from three hard disks (see Fig. 1). An applied magnetic field characterized by the cyclotron radius $R=\hbar k/eB$ is assumed to act inside the region limited by the large circle in Figs. 1 and 2. We restrict ourselves to an arrangement in which the centers of the disks (radius $r_d=1$) form an equilateral triangle of side length $a=2.5$.

The statistical properties of the invariant set (i.e., the set of closed trajectories which never leave the scattering region) corresponding to this arrangement have been investigated and characterized by Breymann *et al.* [16]. For zero and

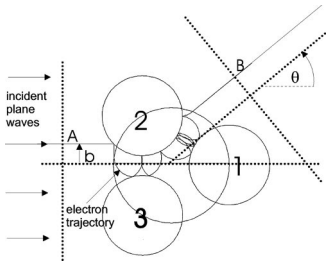

FIG. 1. Scattering geometry for the three-disk billiard. The disks (radius 1) are arranged such that their centers form an equilateral triangle with side length 2.5. The magnetic field with strength $B=mv/eR$ (R is the cyclotron radius) acts only inside the circumferal circle of the triangle (radius R_B).

 ©2000 The American Physical Society

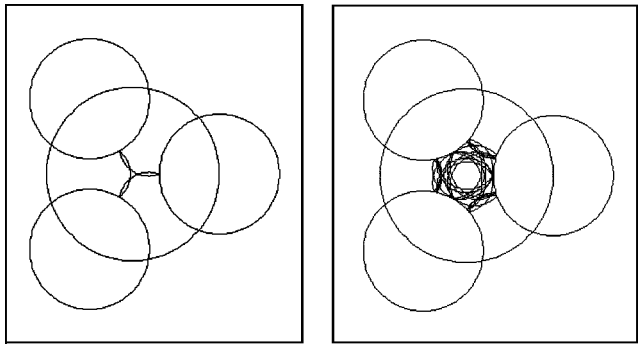

FIG. 2. The shortest stable periodic orbits for cyclotron radius $R=0.5$.

small field the system is fully chaotic (hyperbolic). Beyond a certain critical field (for our geometry $R \leqslant\approx 0.63$, see Appendix A) stable islands appear in the phase space of the invariant set. This drastically influences the scattering properties as evidenced, e.g., by a vanishing escape rate and a vanishing average Lyapunov exponent.

In the following we investigate some features of the nonhyperbolic case in more detail: An important statistical quantity, which will turn out to be relevant for the quantum fluctuations in the semiclassical regime, is the number $N(n)$ of trajectories which are scattered not less than n times. It can also be called the number of trajectories which have not left the scattering region after n bounces or, in short, the survival probability of trajectories. For hyperbolic chaotic scattering systems this quantity is known (e.g., Ref. [18]) to decay exponentially with n, the exponent being the escape rate λ. In the field free case ($R=\infty$) we obtain for the three-disk billiard for our parameters $\lambda=0.48$. We turn now our attention to the case with field corresponding to $R=0.5$ in which stable closed trajectories are present. For the symbolic code of the periodic orbits we use $(-)$ for clockwise scattering, $(+)$ for anticlockwise scattering, and (0) for scattering twice at the same disk. The shortest stable periodic orbits (KAM tori) we found in this case are those with the symbolic code $(-)$ and $(-------0)$, see Fig. 2.

In Fig. 3 we have depicted $N(n)$ of the field-free situation

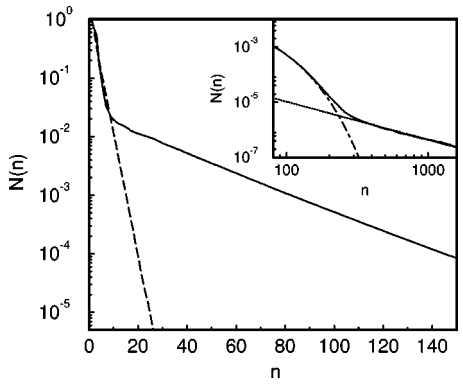

FIG. 3. Survival probability $N(n)$ vs number of reflections n. Dashed line: $R=\infty$ (hyperbolic case). Full line: $R=0.5$ (nonhyperbolic case). For $n>10$ the survival probability decreases exponentially as $N(n)\propto\exp\{-0.48n\}$. Insert: Double-logarithmic plot for $n>100$. The dotted straight line corresponds to $N(n)\propto n^{-1.37}$, the dash-dotted line to $N(n)\propto\exp\{-0.038n\}$.

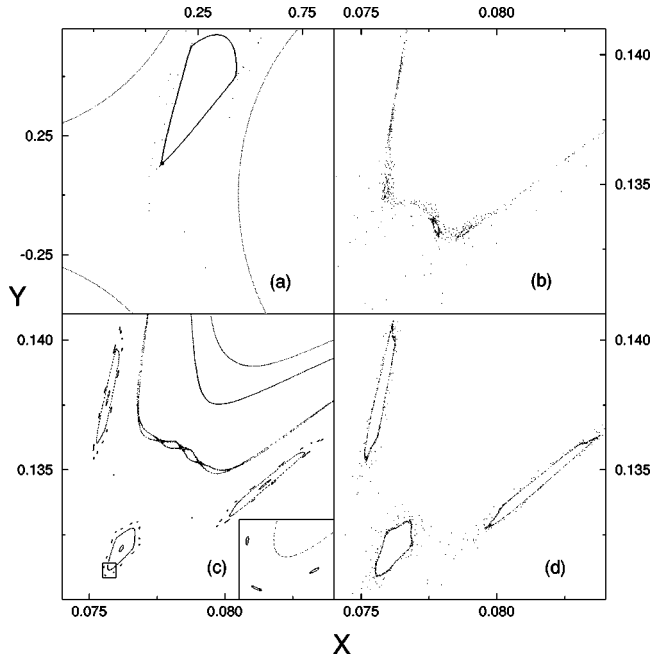

FIG. 4. (a) Midpoints of arcs (phase space portraits) corresponding to two very long trajectories with about 3000 reflections. (b), (d) Magnification of the region around the cusp of the stable island for the two trajectories separately. (c) The invariant set in the phase space region shown in (b) and (d) exhibits a self-similar Poincaré-Birkhoff scenario.

(dashes) together with the function corresponding to $R=0.5$. The latter has, in contrast to the hyperbolic case, an interesting structure. It first decays as the hyperbolic curve until near $n=10$ the presence of the KAM tori becomes distinct. It is well known that the transient trajectories stick a long time near the stable orbits of the invariant set (''stickiness'' of the KAM tori, see e.g., Ref. [10]). This leads to a much slower decay of $N(n)$. It is also known [19–23], that in systems with mixed phase space the survival probability asymptotically decays algebraically according to $N(n)\propto n^{-\beta}$. This is also true in our case (inset of Fig. 3). In the regime $n>300$ an algebraic decay is seen with $\beta=1.37$. In the intermediate range the survival probability decays exponentially with $\lambda=0.038$.

In order to understand this behavior we take a look at the phase space structure of some very long transient trajectories. In Fig. 4 we have plotted the midpoint coordinates X and Y of their cyclotron arcs. These are known to constitute a pair of generalized coordinates which are canonically conjugated with respect to each other. Therefore their loci constitute a Poincaré section. (The Poincaré section is a two-dimensional surface, and the set of all circle midpoints uniquely form this surface.) From Fig. 4(a) it is seen that the long trajectories spend most of their time at the boundary of a stable island, the center of which corresponds to the stable orbit $(-)$. However, at this degree of magnification the self-similar structure of the KAM surface cannot be resolved. This is only the case at a larger magnification (b) and (d). There a typical Poincaré-Birkhoff scenario is visible, which is corroborated by (c), where a Poincaré section of the invariant set is shown. As the algebraic decay of $N(n)$ is a consequence of the fractal remnants of the destroyed tori

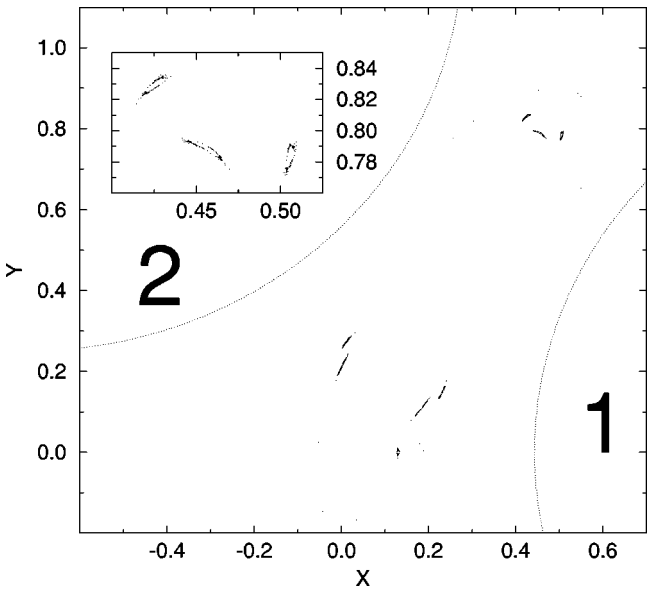

FIG. 5. Phase space portraits of a single long trajectory which follows the stable orbit $(-------0)$ for a long time. The magnification in the insert indicates a Poincaré-Birkhoff scenario.

(''cantori'') at the KAM surface [22], we conclude that the late onset of the algebraic decay follows from the very small phase space volume enclosed by the cantori. For completeness we show in Fig. 5 the Poincaré sections of some long trajectories which follow the stable orbit $(------0)$ (see Fig. 2) for a long time. A Poincaré-Birkhoff scenario is visible as well, but as in the $(-)$ case the phase space volume is tiny.

At the end of this section we would like to comment on the fractal structure of the set of singularities in the scattering function $\tilde{\theta}(b)$, where b is the impact parameter (distance of the incoming ray to the x axis) and $\tilde{\theta}$ is the angle of the outgoing ray with the x axis. It has been postulated [24] that in the case of a mixed phase space the fractal dimension D_0 of this set becomes unity. We have determined the ϵ uncertainty $f(\epsilon)$ [18,24] for the case $R=0.5$, from which D_0 can be determined as $D_0=1-\lim_{\epsilon\to 0}\ln f(\epsilon)/\ln\epsilon$. On a log-log plot of $f(\epsilon)$ [14] we do not find any deviation from a straight line in a range of impact parameter intervals ϵ from 10^{-6} down to 10^{-15}, a resolution at which the survival probability already decays algebraically. The slope yields $D_0=0.89$. We doubt that in our case for smaller intervals a change of the slope from 0.89 to 1 occurs, but, of course, we cannot exclude that this might happen.

III. SEMICLASSICAL TREATMENT OF QUANTUM SCATTERING

For treating the magnetic field inside the central circle of radius r_B quantum mechanically we choose the following gauge for the vector potential $\mathbf{A}(r,\theta)$:

$$\mathbf{A}=\begin{cases}\dfrac{\Phi}{2\pi r}\mathbf{e}_\theta & r\geqslant r_B,\\[2ex] \dfrac{\Phi r}{2\pi r_B^2}\mathbf{e}_\theta & r<r_B.\end{cases} \tag{1}$$

Here $\Phi=B\pi r_b^2$ is the magnetic flux through the central circle and $\mathbf{e}_\theta=\{(-\sin(\theta),\cos(\theta)\}$ is the unit vector in the θ direction. This introduces an additional phase factor in the asymptotic wave functions of the scattering system [25]:

$$\Psi(\theta,r)\overset{r\to\infty}{=}\Psi_{\text{in}}+\Psi_{\text{out}}$$
$$=\exp[-i\alpha(\theta-\pi)]\exp[ik\cos(\theta)r] \tag{2a}$$
$$+\frac{f(\theta)}{\sqrt{r}}\exp(ikr). \tag{2b}$$

$\alpha=e\Phi/hc$ is the number of flux quanta in the central circle.

In semiclassical approximation the scattering amplitude takes the form [26]

$$f(\theta)=\sum_{\tilde{\theta}(b_j)=\theta}\sqrt{c_j}\exp\left[i\left(\frac{\tilde{S}_j}{\hbar}-\frac{\pi}{2}\mu_j\right)\right] \tag{3a}$$

with

$$\tilde{S}_j=\int_A^B\mathbf{p}d\mathbf{q}-\hbar\alpha(\theta_A-\pi)-\alpha\hbar(\theta-\theta_B)-2mwv_0\equiv\hbar k\tilde{L}_j \tag{3b}$$

and

$$c_j=\left|\frac{\partial\tilde{\theta}}{\partial b_j}\right|^{-1}. \tag{3c}$$

The sum in Eq. (3a) has to be performed over all classical trajectories labeled by an impact parameter b_j that are scattered into the same angle θ, i.e., with scattering function [18] $\tilde{\theta}(b_j)=\theta$, $\tilde{S}_j$ is the action integral along a trajectory between the points A and B on the ''start'' and ''goal'' lines (see Fig. 1). $\mathbf{p}=m\mathbf{v}-(e/c)\mathbf{A}$ is the classical canonical momentum. $\tilde{L}$ is an effective length which does not depend on the wave number k. In the absence of the field it is equal to the length of the trajectory. μ_j is the Maslov index [26], which increases by 1 if a caustics is passed, and by 2 in the case of a reflection at one of the disks. The differential cross section is, as in the three-dimensional case, given by

$$\frac{d\sigma}{d\theta}=|f(\theta)|^2. \tag{4}$$

The diagonal term of the resulting double sum gives the classical cross section

$$\left.\frac{d\sigma}{d\theta}(\theta)\right|_{\text{class}}=\sum_{\tilde{\theta}(b_j)=\theta}\left|\frac{\partial\tilde{\theta}}{\partial b_j}\right|^{-1}. \tag{5}$$

Relative extrema in the scattering function $\tilde{\theta}(b)$ lead to ''rainbow'' singularities in the prefactor of the wave function. We have removed these singularities by a cutoff procedure (see Appendix B).

Quantum fluctuations in the scattering amplitude and cross sections appear due to the presence of the phase factors in Eq. (3a). They can be explored by varying an external

parameter, such as the energy of the electrons [Fermi energy $E=(1/2)mv^2=(\hbar k)^2/2m$] or the magnetic field. We choose to study these fluctuations as a function of the wave number k. It has been pointed out by Blümel and Smilanski [4] that the correlation functions that describe the quantum fluctuations are related to the statistics of the classical trajectories in chaotic scattering systems. We are now going to study this relationship in detail for the case of a mixed phase space at cyclotron radius $R=0.5$ and compare it to the hyperbolic case ($R=\infty$). Studying the quantum behavior at different wave numbers with fixed R implies $B/k=$const. k/B can therefore be called the scaled wave number and E/B^2 the scaled energy in the spirit of the scaled field spectroscopy in atomic physics [27]. In order to do so we define the fluctuations of the scattering amplitude and the cross section with the help of an average over a finite k range 2η:

$$\langle f(k)\rangle_\eta=\frac{1}{2\eta}\int_{k-\eta}^{k+\eta}f(k')dk'. \tag{6}$$

The correlation functions of the scattering amplitudes $\tilde{f}_{R\theta}(k)=f_{R\theta}(k)-\langle f_{R\theta}(k)\rangle_\eta$ and the cross sections

$$\widetilde{\frac{d\sigma}{d\theta}}(k)=\frac{d\sigma}{d\theta}(k)-\left\langle\frac{d\sigma}{d\theta}(k)\right\rangle_\eta$$

are then defined as follows:

$$C_{\theta,R,k_0}(\kappa)=\langle\tilde{f}_{R\theta}(k_0)^*\tilde{f}_{R\theta}(k_0+\kappa)\rangle_{\Delta k}, \tag{7a}$$

$$K_{\theta,R,k_0}(\kappa)=\left\langle\widetilde{\frac{d\sigma}{d\theta}}(k_0)\widetilde{\frac{d\sigma}{d\theta}}(k_0+\kappa)\right\rangle_{\Delta k}. \tag{7b}$$

Let us first discuss the correlation function of the scattering amplitude $C_{\theta,R,k_0}(\kappa)$. If Eq. (3a) is inserted into Eq. (7a) a double sum is obtained, the diagonal term of which takes the form

$$C_{\theta,R,k_0}(\kappa)\approx C^d_{\theta,R}(\kappa)=\sum_u \xi^2(\eta\tilde{L}_u)c_u\exp\{i\kappa\tilde{L}_u\}. \tag{8}$$

Here $\xi(x)=1-\sin(x)/x$, coming from the average (6). It is plausible that there should exist a linear relationship between the effective length $\tilde{L}$ of a trajectory and its number n of reflections. We found empirically by plotting $\tilde{L}$ for a large number of trajectories vs n that we have $\tilde{L}\approx\ell n$ with $\ell=0.8$. If we define

$$P_\theta(n):=\sum_j c_j|_{n(j)=n}$$

to be the number of trajectories which are scattered into the angle θ and have exactly n reflections, and if we replace the function ξ by a step function, we have $C^d_{\theta,R}(\kappa)\approx\Sigma_{n=n_0}^{\infty}P_\theta(n)\exp\{i\kappa\ell n\}$, where $n_0>0$ depends on ℓ and η. It is clear that in the case of chaotic scattering (also in the presence of stable orbits) $P_\theta(n)$ only weakly depends on θ. Its angle average, on the other hand, is just $P(n)/2\pi$,

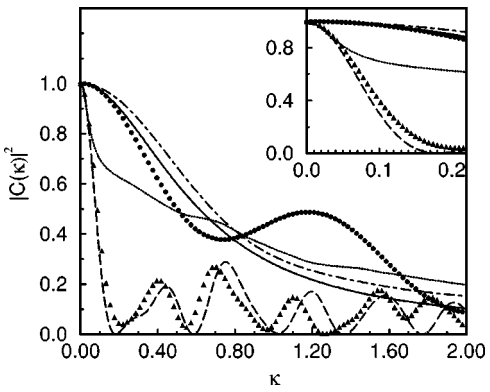

FIG. 6. Modulus square of the correlation function of the scattering amplitude $|C_{\theta,R}(\kappa)|^2$. Full circles: hyperbolic case ($R=\infty$). Triangles: nonhyperbolic case ($R=0.5$). In both cases we chose $\theta=3.4$, $k_0=1000$, $\Delta k=10.0$, $\eta=1.0$. $f_{k,R}(\theta)$ has been evaluated using 2.0×10^7 trajectories from the b interval $[-0.54,0.54]$. For comparison we show $|\Sigma_{n=n_0}^{\infty}P_\theta(n)\exp(i\kappa ln)|^2$ for $R=\infty$ (dash-dotted line) and $R=0.5$ (dashed line) as well as $|\Sigma_{n=n_0}^{\infty}P(n)\exp(i\kappa ln)|^2$ for $R=\infty$ (full line) and $R=0.5$ (small dots) with $l=0.8$ and $n_0=4$. All curves are normalized to unity at $\kappa=0$. The inset shows the small wave number regime, where the striking difference between the hyperbolic and the nonhyperbolic case is most clearly seen.

where $P(n)=N(n)-N(n+1)$ is the total number of trajectories per b interval which undergo n reflections. We can therefore write

$$C^d_{\theta,R}(\kappa)\approx\frac{1}{2\pi}\sum_{n=n_0}^{\infty}P(n)\exp\{i\kappa\ell n\}. \tag{9}$$

It is seen that in this approximation $C_{\theta,R}(\kappa)$ is the Fourier transform of $P(n)$ which is the negative derivative of $N(n)$. This result is similar to that of Blümel and Smilanski [4], who related the energy correlation function of the S-matrix elements to the time dependent survival probability $N(t)$. In the hyperbolic case both $N(n)$ as well as $P(n)$ decay exponentially, so that $|C_{\theta,R}(\kappa)|^2$ becomes a Lorentzian with width λ. As mentioned above, in the case of a mixed phase space $N(n)$ decays asymptotically as $N(n)\propto n^{-\beta}$. Consequently $P(n)\propto n^{-(\beta+1)}$, and the correlation function should then vary as $C_{\theta,R}(\kappa)\propto\kappa^\beta$ [9–12,15]. However in our special case the algebraic behavior sets in only very ''late,'' i.e., after more than 300 bounces.

In Fig. 6 we compare the correlation functions $C_{\theta,R}(\kappa)$ for a arbitrarily chosen angle $\theta=3.4$, which occur in the hyperbolic ($R=\infty$) and in the nonhyperbolic ($R=0.5$) cases. We have added the Fourier transforms of the functions $P(n)$ and $P_\theta(n)$ in order to determine the accuracy of the approximation steps that lead to Eq. (9). The most striking feature is, of course, the different widths of the functions in the different cases. These widths are given by the different escape rates $\lambda=0.48$ and $\lambda=0.038$, respectively. This is plausible from Eq. (9), which states, that the correlation function is essentially the Fourier transform of $P(n)$. It is interesting to note that the diagonal approximation leading to $C_{\theta,R}(\kappa)\approx\Sigma_{n=n_0}^{\infty}P_\theta(n)\exp(i\kappa ln)$ is much more accurate in the non-

hyperbolic case than otherwise. On the other hand $P_\theta(n)$ is very badly approximated by $P(n)$ in this case. Detailed calculations [14] show that the accuracy of the diagonal approximation increases with increasing k_0 and with increasing the smoothing ranges η and Δk.

We turn now to a discussion of the correlation function of the scattering cross section $K_{\theta,R,k_0}(\kappa)$. Inserting Eq. (3a) into Eq. (4), and the result into Eq. (7b) we obtain

$$K_{\theta,R,k_0}(\kappa)=\left\langle \sum_{\substack{u,v,w,z\\ u\neq v,w\neq z}} \sqrt{c_w}\sqrt{c_z}\sqrt{c_u}\sqrt{c_v}\,\xi(\eta[\tilde{L}_u-\tilde{L}_v])\,\xi(\eta[\tilde{L}_w-\tilde{L}_z]) \right. \tag{10a}$$

$$\left. \times\exp[ik(\tilde{L}_w-\tilde{L}_z+\tilde{L}_z+\tilde{L}_u-\tilde{L}_v)]\exp\left[i\frac{\pi}{2}(\mu_w-\mu_z+\mu_u-\mu_v)\right]\exp[i\kappa(\tilde{L}_u-\tilde{L}_v)]\right\rangle_{\Delta\kappa}$$

$$=\underbrace{\sum_{\substack{u,v\\ u\neq v}} c_u c_v\,\xi^2(\eta[\tilde{L}_u-\tilde{L}_v])\exp\left\{i\kappa[\tilde{L}_u-\tilde{L}_v]\right\}}_{K^d_{\theta,R}(\kappa)} + \left\langle \sum_{\substack{u,v,w,z\\ u\neq v,w\neq z\\ u\neq z,w\neq v}} \cdots \right\rangle_{\Delta k} \tag{10b}$$

where $K^d_{\theta,R}(\kappa)$ is the diagonal part. If we compare it with the diagonal part (8) of the scattering amplitude correlation function we see that we have approximately $K^d_{\theta,R}(\kappa)\approx|C^d_{\theta,R}(\kappa)|^2$. The difference consists in a different combination of the ξ functions. In Eq. (10b) the effect of these functions is to eliminate those pairs of trajectories which have an effective length difference larger than $1/\eta$, whereas in Eq. (8) the ξ functions eliminate short trajectories. Neglecting these different restrictions we can state in diagonal approximation

$$K^{\theta,R}(\kappa)\approx|C^{\theta,R}(\kappa)|^2. \tag{11}$$

In Fig. 7 we compare the correlation functions of the scattering cross sections in the hyperbolic ($R=\infty$) and nonhyperbolic case ($R=0.5$) with $|C^{\theta,R}(\kappa)|^2$. We have also taken two different angles θ to show the weak but distinct angle dependence of the fluctuations. Since the cross sections of our model geometry can approximately be related to the transmission coefficients in a three-lead junction we expect that the results shown in Fig. 7 should be similar to the mesoscopic fluctuations of the conductance of a three-lead junction with and without a magnetic field. As soon as stable classical orbits appear the range and the degree of correlation of the fluctuations change drastically. Again the small-κ regime is characterized by the different escape rates of Fig. 3. Furthermore we observe in the nonhyperbolic case at higher wave numbers characteristic oscillations which are absent in the hyperbolic case.

In the following we are going to demonstrate that these oscillations are due to a Bohr-Sommerfeld type quantization of the stable periodic orbits. From Eq. (10b) it follows that $K^{\theta,R}(\kappa)$ is essentially the Fourier transform of the weights $c_u c_v$ with respect to the effective length differences $\tilde{L}_u-\tilde{L}_v$. This product can be interpreted as the probability for a pair of trajectories (u,v) having the effective lengths $\tilde{L}_u$ and $\tilde{L}_v$. In Figs. 8 and 9 we compare the Fourier transform of $K^{\theta,R}(\kappa)$ (form factor) with a plot of the products $c_u c_v$ against the modulus of effective length difference. In the hyperbolic case the form factor decays rapidly and has a random structure. In the nonhyperbolic case the form factor decays very slowly and has a periodic structure. This structure is also visible in the values of the weights $c_u c_v$. The

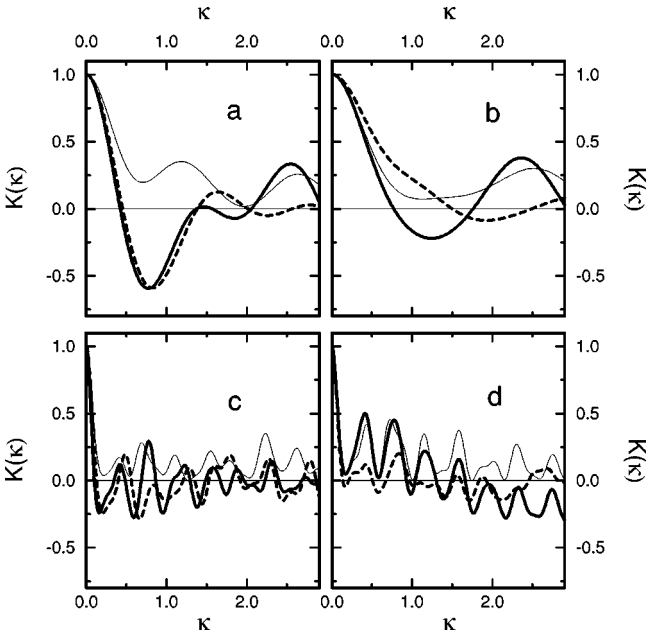

FIG. 7. Correlation function of scattering cross sections. (a) and (b) hyperbolic case ($R=\infty$), (c) and (d) nonhyperbolic case ($R=0.5$). The averages in (a) and (c) have been done with $\eta=1$ and $\Delta k=30$, whereas in (b) and (d) with $\eta=30$ and $\Delta k=30$. Full thick lines correspond to scattering cross sections into angle $\theta=3.4$, dashed lines $\theta=5.4$, thin lines are $|C^{\theta,R}(\kappa)|^2$.

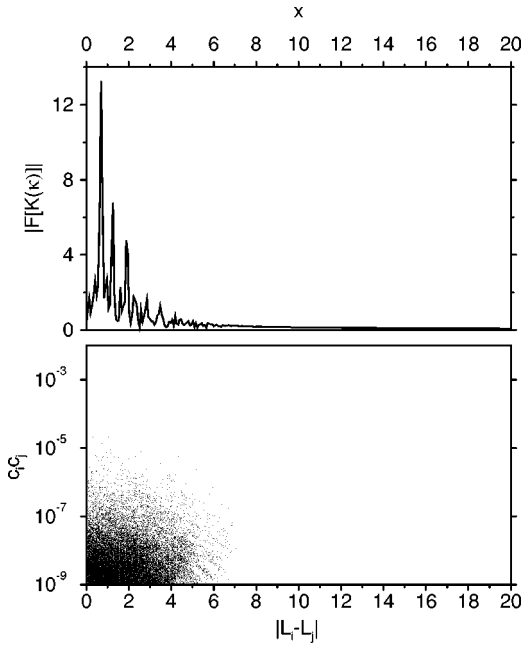

FIG. 8. Fourier transform of the cross-section correlation function (form factor) vs orbit length difference $L_i - L_j$ together with the values of $c_i c_j$ used for calculating $K^{\theta,R}(\kappa)$ for the hyperbolic case $(R=\infty)$.

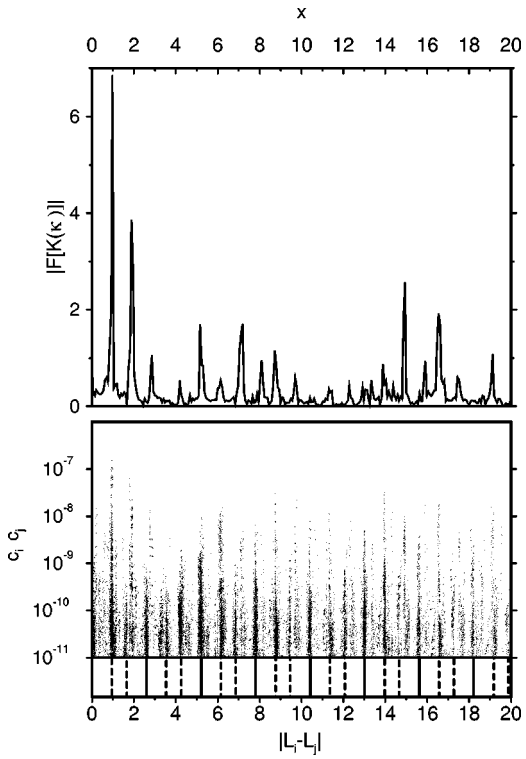

FIG. 9. Fourier transform of the cross-section correlation function (form factor) vs effective length difference $\tilde{L}_i - \tilde{L}_j$ together with the values of $c_i c_j$ used for calculating $K^{\theta,R}(\kappa)$ for the nonhyperbolic case $(R=0.5)$. The bottom picture shows full rectangular lines at length differences being multiples of $L_- = 2.6$ [effective length of the stable orbit (/) of Fig. 2]. The positions of the broken lines are those of the full lines plus and minus L_{+-} [effective length of the unstable periodic orbit $(+-)$ (see the Appendix)].

period is just the effective length $\tilde{L}_- = 2.6$ (see Appendix A). There is an additional structure within the period of the stable orbits which just corresponds to a length of the unstable orbit $(+-)$, $L_{+-} = 0.96$. It seems that the transient orbits, when they enter or leave the vicinity of the stable orbits of the $(-)$ type have sections of the $(+-)$ type. Thus, we find that the periodic structure in the correlation function of the scattering cross section is due to resonances which appear if the Bohr-Sommerfeld condition

$$\hbar k \tilde{L}_- = \oint \mathbf{p} d\mathbf{q} = 2\pi\hbar(n+c) \tag{12}$$

for quantization of the stable orbit $(-)$ is fulfilled.

IV. DISCUSSION AND CONCLUSION

We have studied the classical and quantum chaotic scattering properties of the three-disk billiard in the absence and presence of an applied magnetic field. In the absence of the field the system is hyperbolic and exhibits an exponentially decaying survival probabiliby $N(n)$ of trajectories in the scattering region. Beyond a certain critical field some of the invariant orbits become stable, which leads to a much slower decrease of $N(n)$. The asymptotic algebraic decay with exponent $\beta = 1.37$ is reached only for $n > 300$. The drastic change in the statistics of the transient trajectories is reflected in the statistics of the quantum fluctuations. As the correlation function $C(\kappa)$ of the wave number fluctuations of the scattering amplitude is approximately proportional to the Fourier transform of the derivative of $N(n)$, the slow decay of $N(n)$ is reflected in a much sharper peak in $|C(\kappa)|^2$ near $\kappa = 0$. The latter quantity is, in diagonal approximation, approximately proportional to the correlation function $K(\kappa)$ of the wave number fluctuations of the cross section. This effect should be visible in three- or four-lead junctions under the influence of an applied magnetic field.

In our case the phase space enclosed by the the fractal ''cantori'' is very small and is only explored by very long transient classical trajectories. Their role in the quantum fluctuations is negligible. Therefore for our model the quantum fluctuations are not self-similar as is the case for other scattering geometries with mixed phase space [11,15,28–30]. Whether or not this situation is exceptional or generic in systems with mixed phase space must be explored by further model calculations and experimental measurements.

In our semiclassical calculation the phase space structure of the trapped orbits enter via the transient orbits. Recently a theoretical investigation was published in which the quantum time delay is directly related to a semiclassical sum over the closed orbits of the scattering region [8]. One can therefore expect that the fluctuations in the quantum time delay will reflect the phase space structure of the invariant set in a similar way as it is the case for the fluctuations of the transmission coefficients. We conclude by suggesting to measure the conductance fluctuations of rounded junctions at different scaled fields to detect the traces of the transition from the hyperbolic to the nonhyperbolic situations.

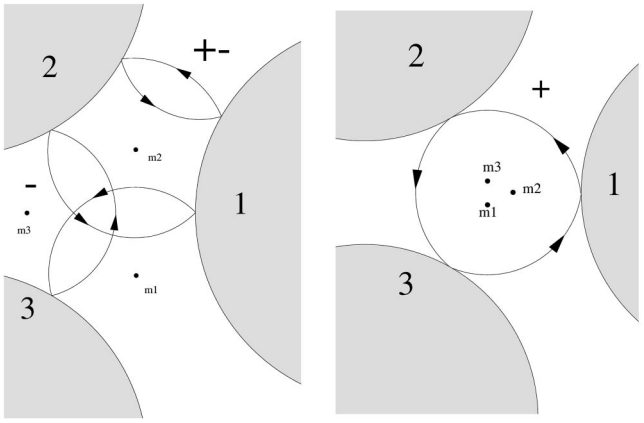

FIG. 10. Left: The unstable periodic orbit with code $(+-)$ and the simplest of the stable periodic orbits with code $(-)$ together with the midpoints m_i of the arcs. m_2 is in the center of the stable island in Fig. 4. Right: The simplest of the unstable periodic orbits with code $(+)$.

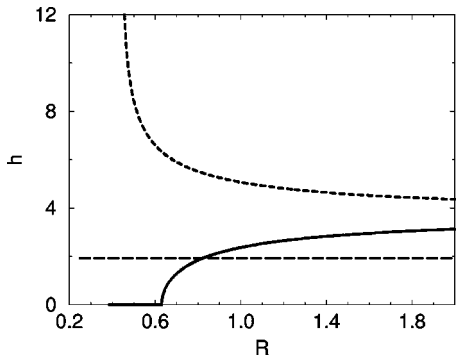

FIG. 11. Lyapunov exponents h for the unstable orbits depicted in Fig. 11 as a function of the cyclotron radius R.

ACKNOWLEDGMENTS

We are indebted to H. Thomas and H. Friedrich for continuous support and stimulating discussions. W. S. is grateful to J. Hajdu for hospitality at Cologne University. This work has been supported by Deutsche Forschungsgemeinschaft under Schi 308/4-1.

APPENDIX A: THE SMALLEST CLOSED ORBITS OF THE THREE-DISK BILLARD

The Poincaré map $\mathcal{K}_i$ which generates the sequence of midpoint coordinates (m_x, m_y) of arcs due to reflections from disk # i with midpoint (x_i, y_i) is given by

$$m_x' = s_x + (m_x - x_i)\cos(2\gamma) - (m_y - y_i)\sin(2\gamma),$$

$$m_y' = s_y + (m_x - x_i)\sin(2\gamma) + (m_y - y_i)\cos(2\gamma). \quad \text{(A1)}$$

It is just a rotation about (x_i, y_i) by the angle γ defined by

$$\cos(\gamma) = \frac{r_d^2 + d^2 - R^2}{2 r_d d}$$

with

$$d = \sqrt{(m_x - s_x)^2 + (m_y - s_y)^2}.$$

The stability of an orbit of period p is determined by the eigenvalues $\lambda_\pm$ of the stability matrix $\mathbf{S} = (D\mathcal{K}_i)^p$ which is the pth power of the Jacobian of $\mathcal{K}_i$. In terms of the trace T of $\mathbf{S}$ they are given by [16]

$$\lambda_\pm = \frac{1}{2}(T \pm \sqrt{T^2 - 4}). \quad \text{(A2)}$$

Since $\lambda_+ \lambda_- = 1$ they are either unit roots (stable case, $|T| < 2$) or real and reciprocal to each other. The Lyapunov exponent h is then given by the greater of the two as $h = \ln|\lambda_+|$. In Fig. 10 we show the Lyapunov exponents of the three periodic orbits depicted in Fig. 11.

For the effective lengths of these orbits we have to calculate the action along the orbit

$$\hbar k \tilde{L} = S = \oint b f p d i b f q = \hbar k l - \frac{e_0}{c} B F = \hbar k \left(l - \frac{F}{R} \right), \quad \text{(A3)}$$

where l is the length of the periodic orbit and F the oriented net area.

For the orbits $(+)$ and $(-)$ we obtain

$$\tilde{L}_\pm = 3Rw + \frac{1}{R}(3z\sqrt{R^2 - z^2} \mp z^2\sqrt{3}) \quad \text{(A4a)}$$

with

$$z = \frac{a - \sqrt{3}}{2} \quad \text{and} \quad w = \arcsin\left(\frac{z}{R}\right). \quad \text{(A4b)}$$

For the orbit $(+-)$ we have

$$\tilde{L}_{+-} = 2R \arcsin\left(\frac{\tilde{z}}{R}\right) + 2\tilde{z}\sqrt{1 - \frac{\tilde{z}^2}{R^2}} \quad \text{(A5a)}$$

with

$$\tilde{z} = \frac{a}{2} - 1. \quad \text{(A5b)}$$

APPENDIX B: RAINBOW SINGULARITIES

A rainbow singularity appears if the scattering function $\tilde{\theta}(b)$ has an extremum at a certain value θ_s. If we add the semiclassical scattering amplitudes on both sides of the extremum we get [14]

$$f_s(\theta) = \exp(i\delta)\frac{\sqrt{2}}{\sqrt{|A|}}\left(\frac{\theta - \theta_s}{A}\right)^{-1/4} \times \cos\left(k\frac{2}{3}|AB|\left(\frac{\theta - \theta_s}{A}\right)^{3/2} - \frac{\pi}{4}\right), \quad \text{(B1)}$$

with $A = \frac{1}{2}(\partial^2\theta/\partial^2 b)$, $B = (\partial\tau/\partial b)$ and $\delta = k\tilde{L}_s - \pi/4(\mu_+ + \mu_-)$. Here τ is the impact parameter along the ''goal

line'' at point B (see Fig. 1). This expression, which diverges at θ_s is regularized in the usual way [21] by means of the Airy function $\mathrm{Ai}(x)$:

$$f_s(\theta)=\exp(i\delta)\frac{\sqrt{2\pi}}{\sqrt{|A|}}|kAB|^{1/6} \times \mathrm{Ai}\left[-|kAB|2/3\,\frac{\theta-\theta_s}{A}\right]. \tag{B2}$$

The bookkeeping of these expressions takes a lot of computing time. So we replaced in our numerical calculations $\tilde{\theta}(b)$ by 10^{-40} in the region around θ_s, where $\tilde{\theta}(b)<10^{-40}$. We compared calculations using this cutoff procedure with calculations using Eq. (B2), where we took an approximate version of the Airy function [14]. We found only minor differences, and the statistical properties of the results were not altered. We therefore used the cutoff procedure throughout our calculations.

[1] C. W. J. Beenakker and H. van Houten, in *Solid State Physics*, edited by H. Ehrenreich and D. Turnbull (Academic Press, Inc., San Diego, 1991), Vol. 1, pp. 1–228.

[2] *Mesoscopic Quantum Physics*, edited by E. Akkermans, G. Montambaux, J.-L. Pichard, and J. Zinn-Justin (North-Holland, Amsterdam, 1995).

[3] *Chaos and Quantum Physics*, edited by M. J. Giannoni, A. Voros, and J. Zinn-Justin (North-Holland, Amsterdam, 1991).

[4] R. Blümel and U. Smilansky, Phys. Rev. Lett. **60**, 477 (1988).

[5] R. A. Jalabert, H. U. Baranger, and A. D. Stone, Phys. Rev. Lett. **65**, 2442 (1990); **60**, 477 (1988).

[6] A. D. Stone in Ref. [2].

[7] C. M. Marcus, A. J. Rimberg, R. M. Westervelt, P. F. Hopkins, and A. C. Gossard, Phys. Rev. Lett. **69**, 506 (1992).

[8] R. O. Vallejos, A. M. Ozorio de Almeida, and C. H. Lewenkopf, J. Phys. A **31**, 4885 (1998).

[9] Y. Lai, R. Blümel, E. Ott, and C. Grebogi, Phys. Rev. Lett. **68**, 3491 (1992).

[10] Y. Lai, M. Ding, C. Grebogi, and R. Blümel, Phys. Rev. A **46**, 4661 (1992).

[11] R. Ketzmerick, Phys. Rev. B **54**, 10 841 (1996).

[12] M. Eichengrün, W. Schirmacher, and W. Breymann, Europhys. Lett. **36**, 483 (1996).

[13] M. Eichengrün, W. Schirmacher, and W. Breymann, Phys. Status Solidi B **205**, 219 (1998).

[14] M. Eichengrün, doctoral dissertation, Techn. Univ. München, 1997.

[15] A. S. Sachrajda *et al.*, Phys. Rev. Lett. **80**, 1948 (1998).

[16] W. Breymann, Z. Kovacs, and T. Tel, Phys. Rev. E **50**, 1994 (1994).

[17] B. Eckhard, J. Phys. A **20**, 5971 (1987).

[18] E. Ott, *Chaos in Dynamical Systems* (Cambridge University Press, Cambridge, 1993).

[19] J. D. Meiss, J. R. Cary, C. Grebogi, J. D. Crawford, A. N. Kaufmann, and H. D. Abarbanel, Physica D **6**, 375 (1983).

[20] C. F. F. Kurney, Physica D **8**, 360 (1983).

[21] B. V. Chirikov and D. L. Shepelyansky, Physica D **13**, 395 (1984).

[22] J. D. Meiss and E. Ott, Phys. Rev. Lett. **55**, 2741 (1985).

[23] M. Ding, T. Bountis, and E. Ott, Phys. Lett. A **151**, 395 (1990).

[24] Y. T. Lau, J. M. Finn, and E. Ott, Phys. Rev. Lett. **66**, 978 (1991).

[25] M. Peshkin and A. Tonomura, *The Aharonov-Bohm Effect* (Springer-Verlag, Berlin, 1989).

[26] V. P. Maslov and M. V. Fedoriuk, *Semiclassical Approximation in Quantum Mechanics* (Reidel, Boston, 1981).

[27] H. Friedrich, in *Atoms and Molecules in Strong External Fields*, edited by P. Schmelcher and W. Schweizer (Plenum Press, New York, 1998), p. 153. See also the articles of J. Main, J. B. Delos, and C. Schwieters, in *Classical, Semiclassical and Quantum Dynamics in Atoms*, edited by H. Friedrich and B. Eckhardt, Vol. 485 of Lecture Notes in Physics (Springer-Verlag, Heidelberg, 1997), pp. 274 and 232.

[28] R. P. Taylor, R. Newbury, A. S. Sachrajda, Y. Feng, P. T. Coleridge, C. Dettmann, N. Zhu, H. Guo, A. Delage, P. J. Kelly, and Z. Wasilewski, Phys. Rev. Lett. **78**, 1952 (1997).

[29] R. P. Taylor, A. P. Micolich, R. Newbury, and T. M. Fromhold, Phys. Rev. B **56**, R12 733 (1997).

[30] R. P. Taylor, A. P. Micolich, R. Newbury, J. P. Bird, T. M. Fromhold, J. Cooper, Y. Aoyagi, and T. Sugano, Phys. Rev. B **58**, 11 107 (1998).